Science of the Total Environment 784 (2021) 147151

Contents lists available at ScienceDirect

Science of the Total Environment

journal homepage: www.elsevier.com/locate/scitotenv

A compartmentalized microsystem helps understanding the uptake of benzo[*a*]pyrene by fungi during soil bioremediation processes

Claire Baranger [a], Isabelle Pezron [a], Laurence Lins [b], Magali Deleu [b], Anne Le Goff [c,*], Antoine Fayeulle [a,*]

[a] Université de technologie de Compiègne, ESCOM, TIMR (Integrated Transformations of Renewable Matter), Centre de Recherche Royallieu - CS 60 319 - 60 203 Compiègne Cedex, France
[b] TERRA Research Center, Laboratory of Molecular Biophysics at Interfaces, SFR Condorcet, Gembloux Agro-Bio Tech, University of Liege, Passage des Déportés, 2, 5030 Gembloux, Belgium
[c] Université de technologie de Compiègne, CNRS, Biomechanics and Bioengineering, Centre de recherche Royallieu - CS 60 319 - 60 203 Compiègne Cedex, France

HIGHLIGHTS

- A compartmentalized microchip was developed to grow the fungus *Talaromyces helicus*.
- The microchip enables to observe how the fungus reach benzo[*a*]pyrene (BaP).
- BaP is incorporated into the cells of *T. helicus* in lipid bodies.
- BaP uptake occurs even when hyphae are not in direct contact with BaP crystals.
- *T. helicus* produces extracellular non lipidic surface-active compounds.

GRAPHICAL ABSTRACT

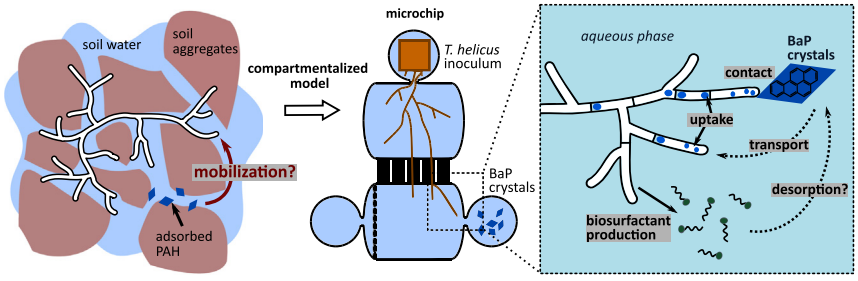

ARTICLE INFO

Article history:
Received 22 January 2021
Received in revised form 1 April 2021
Accepted 11 April 2021
Available online 17 April 2021

Editor: Fang Wang

Keywords:
Bioavailability
Biodegradation
Biosurfactant
Microfluidic device
Mycoremediation
Polycyclic aromatic hydrocarbons

ABSTRACT

Hydrophobic organic soil contaminants such as polycyclic aromatic hydrocarbons (PAH) are poorly mobile in the aqueous phase and tend to sorb to the soil matrix, resulting in low bioavailability. Some filamentous fungi are efficient in degrading this kind of pollutants. However, the mechanism of mobilization of hydrophobic compounds by non-motile microorganisms such as filamentous fungi needs investigations to improve pollutant bioavailability and bioremediation efficiency. Usual homogeneous media for microbial growth in the lab are poorly suited to model the soil, which is a compartmentalized and heterogeneous habitat.

A microfluidic device was designed to implement a compartmentalization of the fungal inoculum and the source of the pollutant benzo[*a*]pyrene (BaP) as a deposit of solid crystals in order to gain a further insight into the mechanisms involved in the access to the contaminant and its uptake in soils. Thus in this device, two chambers are connected by an array of parallel microchannels that are wide enough to allow individual hyphae to grow through them. Macro-cultures of *Talaromyces helicus* in direct contact with BaP have shown its uptake and intracellular storage in lipid bodies despite the low propensity of BaP to cross aqueous phases as shown by simulation. Observations of *T. helicus* in the microfluidic device through laser scanning confocal microscopy indicate preferential uptake of BaP at a close range and through contact with the cell wall. However faint staining of some hyphae before contact with the deposit also suggests an extracellular transport phenomenon. Macro-culture filtrates analyses have shown that *T. helicus* releases extracellular non-lipidic surface-active compounds able to lower the surface tension of culture filtrates to 49.4 mN/m. Thus, these results highlight the significance of active mechanisms to reach hydrophobic contaminants before their uptake by filamentous fungi in compartmentalized micro-environments and the potential to improve them through biostimulation approaches for soil mycoremediation.

* Corresponding authors.
E-mail addresses: anne.le-goff@utc.fr (A. Le Goff), antoine.fayeulle@utc.fr (A. Fayeulle).

https://doi.org/10.1016/j.scitotenv.2021.147151
0048-9697/

1. Introduction

Soil is a complex environmental compartment resulting from the weathering of parental rock under the combined action of living organisms, surface water and the atmosphere. As a support for human activities, soil is heavily affected by pollution and notably with persistent pollutants, which is a major source of soil quality alteration (Panagos et al., 2013). Among these pollutants, some families of organic contaminants including polycyclic aromatic hydrocarbons (PAH), polychlorobiphenyls, and various xenobiotics and pesticides, are highly hydrophobic and persistent in soils. Due to their carcinogenicity and high persistence in the environment, PAH are among the most regulated pollutants in environmental policies (Jennings, 2012). Such poorly water-soluble contaminants can be present in non-aqueous-phase liquids, tar or solid particles. Moreover, they tend to strongly sorb to soil aggregates and organic matter (Ortega-Calvo et al., 2013). These properties make them poorly available for degradation by microorganisms (Posada-Baquero et al., 2019).

Bioremediation corresponds to the use of biological activities in particular of microorganisms to destroy pollutants or decrease the associated risks for humans and the environment. It is regarded as a low-technology and low-cost approach with a higher degree of public acceptance in comparison to other physicochemical remediation techniques more destructive of the living fraction and the structure of soils such as high temperature incineration, chemical decomposition, solvent extraction or UV oxidation (Vidali, 2001). Thus bioremediation is one of the established methods undergoing the highest development for PAH cleanup in soils (Kuppusamy et al., 2017). One of the parameters that can impair bioremediation efficiency is the low competitiveness and adaptability of microbial inocula (Rayu et al., 2012), which could be prevented by the use of telluric strains. Soil is a divided environment consisting in solid, aqueous and gas phases, hosting a great variety of living organisms, including fungi. Among microorganisms, micromycetes are particular in the sense that they do not need water as a support for dispersal, and can form aerial structures. This allows mycelium to occupy vast volumes of soil and come into contact with several phases. Indeed, soil fungi are known for their ability to form mycelial networks in three dimensions that constitute large exchange surfaces within the soil porosities, and to mobilize nutritious substrates through the release of extracellular lytic enzymes before substrates incorporation (Moore et al., 2015). Notably, micromycetes play important roles in hydrophobic organic pollutants dynamics within the soil matrices (Baranger et al., 2021).

Hydrocarbons can be a source of carbon and energy for fungi. In non-ligninolytic fungi, the main metabolic pathway described as involved in PAH biodegradation is the cytochrome P450 pathway. Cytochrome P450 mono-oxygenases are a family of intracellular enzymes involved in the oxidation of various hydrophobic substrates (Črešnar and Petrič, 2011). Cytochrome P450 monooxygenases initiate the oxidation of PAH into arene oxides that are further metabolized into phenol and dihydrodiol derivatives (Cerniglia and Sutherland, 2010). This intracellular degradation pathway implies preliminary uptake of hydrocarbons and notably PAH by fungal cells.

Lindley and Heydeman (1986) first described the incorporation of dodecanol into whole cells of *Cladosporium resinae* by early adsorption to the cell surface followed by active uptake. More recent studies have focused on the uptake of various hydrophobic organic pollutants including polycyclic aromatic hydrocarbons (PAH). PAH have been described to behave in a similar way to neutral lipids, diffusing into lipid membranes (Castelli et al., 2002) and being incorporated in lipid storage sites in fungal cells (Verdin et al., 2005; Chang et al., 2015). Notably, the ubiquitous PAH benzo[*a*]pyrene (BaP) can be localized in lipid bodies in mycelium that has been cultivated in contact with this pollutant (Verdin et al., 2005; Fayeulle et al., 2014). However, an active transport mechanism for BaP uptake dependent on the fungal cytoskeleton has been highlighted in *Fusarium solani*, and active phenomena may be involved in BaP mobilization before its uptake by the same fungus (Fayeulle et al., 2014). Interestingly, an active secondary transport mechanism was recently proposed for the uptake of monoaromatic compounds by *Phanerochaete chrysosporium* (Leriche-Grandchamp et al., 2020).

Some micro-organisms are able to release biosurfactants, which can partially solubilize hydrophobic substrates and have been studied for the dispersal of hydrocarbons. In fungi, biosurfactants and emulsifiers are involved in nutrition for the mobilization of fats and adhesion to hydrophobic surfaces (Käppeli et al., 1984). Modulations of cell surface hydrophobicity drive the attachment to surfaces and utilization of hydrophobic substrates (plant leaf wax, oils…) and can affect the fungal interaction with hydrophobic pollutants (Puchkov et al., 2002; Arutchelvi et al., 2008; Garay et al., 2018). Adsorption of hydrophobic substrates on the cell surface is thus thought to be a determining step prior to potential uptake by the cells (Fayeulle, 2013; Al-Hawash et al., 2019). It is known that surfactants are released in the aqueous phase and accumulate at solid/water and air/water interfaces. However the interaction of fungal surfactants with hydrophobic soil contaminants and their potential contribution to pollutant mobilization is poorly understood.

Talaromyces helicus is a filamentous soil ascomycete with a cosmopolitan distribution, found on several continents in temperate to tropical climates (Huang and Schmitt, 1975; Romero et al., 2009; Scervino et al., 2010; Olagoke, 2014; Wu et al., 2016; Fayeulle et al., 2019). It can grow at moderate temperatures (20 °C) and presents relatively fine hyphae of 1 to 3 μm in diameter (Baranger et al., 2020) able to penetrate microporosities and narrow cracks in the substrate, thus potentially covering large volumes of soil. This species has been isolated from contaminated soils, showing the resistance of some strains to pollutions, and its adaptation to the soil environment (Fayeulle et al., 2019). Thus, *T. helicus* has been identified as holding potential for the bioremediation of multiple contaminations due to the bioaccumulation of heavy metals and the biodegradation of several organic pollutants including isoproturon, biphenyl and benzo[*a*]pyrene (Romero et al., 2005, 2009, 2010; Fayeulle et al., 2019). The particular efficiency of *T. helicus* to improve PAH biodegradation in industrial soils with aged mixed contaminations was also highlighted at the microcosm scale (Fayeulle et al., 2019).

In this study, we aim to investigate the biodegradation of BaP by *T. helicus* at the microscopic scale, which corresponds both to the size of fungal hyphae and to that of soil aggregates, and is therefore a natural scale to study soil microbial processes (Wilpiszeski et al., 2019). Microfluidics offer the possibility to design model microenvironments with a good control of their geometry and chemical properties, taking advantage of the specific properties of small scale fluid flows to finely tune mechanical forces and mass transfers (Squires and Quake, 2005). Transparent microfluidic devices, usually made of glass or silicon rubber, can be used as soil models (Aleklett et al., 2018) and accommodate the growth of plant roots (Grossmann et al., 2011), bacterial communities (Alnahhas et al., 2019) or fungi (Held et al., 2010). Parameters such as hyphal growth velocity can be measured by videomicroscopy and can be used to assess the ability of a fungal strain to colonize a polluted porous matrix (Baranger et al., 2020).

In this work, we used a microfluidic device in which the model pollutant and the fungus were introduced in two separate compartments. The aim of such an experiment is to elucidate whether a filamentous fungus needs to grow in contact to the pollutant source for its uptake and degradation, or whether prior extracellular mobilization mechanisms are required to enhance the pollutant bioavailability in the aqueous phase. The investigation of this biological process is important for future optimizations of PAH mycoremediation protocols in soils through biostimulation approaches. This study is the first one to our knowledge to use a microfluidic device in order to understand pollutants mobilization mechanisms by micromycetes in soil.

2. Materials and methods

2.1. Fungal strain

A strain of the filamentous fungus *Talaromyces helicus* from our laboratory collection and previously isolated from an industrial contaminated soil from North of France was used for this study. Identification of the strain occurred through molecular approach by BCCM™/MUCL (Louvain-la-Neuve, Belgium) based on sequencing ITS region, elongation factor gene, or β-tubulin gene, in complement of the macro- and micro-morphological features of pure cultures. The strain was maintained on MYEA solid medium (malt extract 20 g/L – Condalab, Madrid, Spain; yeast extract 2 g/L – VWR, Fontenay-sous-Bois, France; microbiological grade agar 15 g/L – Becton Dickinson, Rungis, France), at 22 °C with a 12 h - 12 h light-dark cycle, and transplanted onto fresh medium every ten days.

Fresh mycelium was produced in a rich medium (MYPC) containing malt extract 10 g/L, yeast extract 4 g/L, soy peptone 10 g/L (Merck, Darmstadt, Germany) and casamino-acids 2 g/L. Shaking flasks containing 50 mL MYPC were inoculated with spores of *T. helicus* to reach a final concentration of 10^4 spores/mL.

2.2. Off-chip incubation with benzo[a]pyrene and lipid staining

T. helicus cultures with BaP were prepared in mineral medium supplemented with glucose (MMG) at pH 5.5, as described by Fayeulle et al. (2019). MMG is comprised of KCl 0.25 g/L, $NaH_2PO_4 \cdot 2H_2O$ 1.54 g/L, Na_2HPO_4 8 mg/L, $MgSO_4 \cdot 7H_2O$ 0.25 g/L, NH_4NO_3 1 g/L, $ZnSO_4 \cdot 7H_2O$ 1 mg/L, $MnCl_2 \cdot H_2O$ 0.1 mg/L, $FeSO_4 \cdot 7H_2O$ 1 mg/, $CuSO_4 \cdot 5H_2O$ 0.5 mg/L, $CaCl_2 \cdot 2H_2O$ 0.1 mg/L, MoO_3 0.2 mg/L and glucose 20 g/L. Mineral salts and glucose were purchased from Thermo Fisher Scientific (Illkirch-Graffenstaden, France). Prior to adding the medium, 50 μg of BaP (Sigma-Aldrich, Haverhill, United Kingdom) was introduced in each flask by pipetting the correct amount of a BaP stock solution in acetone (0.8 g/L), and allowing the acetone to evaporate under a fume hood. Shaking flasks were inoculated with fresh mycelium of *T. helicus* that was pre-grown in MYPC, and were then incubated for 24 h. After incubation, mycelium pellets were mounted on a microscope slide and observed in bright field and epifluorescence microscopy or in laser scanning confocal microscopy.

Lipids were stained in vivo on fresh mycelium samples taken from liquid cultures, using BODIPY 500/510 lipid dye (Thermo Fischer Scientific – Illkirch-Graffenstaden, France). The stock solution of BODIPY in DMSO was pipetted directly onto mycelium samples mounted on a glass microscope slide, achieving a final dye concentration of 0.1 μM/mL.

2.3. Production and detection of surface-active compounds

Shaking flasks containing MMG were inoculated with spores of *T. helicus* to reach a final concentration of 10^4 spores/mL. 50 mL flasks containing 10 mL medium were used for the growth kinetics experiment, and 250 mL flasks containing 50 mL medium were used for filtrates production before characterization. Cultures were incubated at 22 °C with orbital shaking and a 12 h/12 h light-dark cycle. The mycelium was harvested by vacuum-filtration on quantitative filter paper (VWR 434) with a Büchner funnel. Filtrates were collected, filtered again on a 0.2 μm syringe filter to sterilize them and remove any remaining particle, and frozen at −20 °C until use. To quantify fungal growth in 10 mL cultures, the paper filters with mycelium cake were rinsed with distilled water and dried in a 105 °C oven for 24 h, then weighted. For the growth kinetics experiments, 10 mL cultures were done in triplicate and filtered separately.

Surface tension in filtrates was measured on a tensiometer (Krüss K-100) with the Wilhelmy plate method. Each measurement was taken 10 min after immersing the plate into the sample, to allow the meniscus to equilibrate at room temperature. All measurements were performed on triplicate samples, and results are presented as average values and standard deviations for each triplicate.

2.4. High-performance thin-layer chromatography

High-Performance Thin-Layer Chromatography (HPTLC) analysis of culture filtrates was conducted by the CAP DELTA laboratory at Chromacim (Grabels, France) with the CAMAG method. Soy lecithin (1 g/L), bovine serum albumin (1 g/L) and glucose (1 g/L) were used as positive controls for the detection of lipids, proteins and reducing sugars respectively. 10 μL of each control was deposited on the plate, as well as 50 μL of the crude filtrate. Samples were deposited on a TLC plate coated with F254 silica gel with an application spray ATS 4 and migrated vertically in a saturated ADC2 chamber over 20 min (migration distance of 70 mm). The mobile phase was a cosolvent mixture containing $CHCl_3$: CH_3OH:H_2O:NH_3 32% (32:15:2:1 in volume).

After migration, thin layer plates were imaged under white light, UV 254 nm, UV 366 nm and scanned at 200 nm. Then a revelation was done with a primulin reagent (0.1 g/L in acetone:water 80:20 by volume) before imaging under white light, UV 366 nm and scanning at 366 nm for the detection of aliphatic carbon chains corresponding to lipids. Finally a revelation with an anisaldehyde reagent (4-methoxybenzaldehyde at 0.5% *v*/v in CH_3OH:CH_3COOH:H_2SO_4 42.5:5:2.5 by volume) was carried out as well as imaging under white light and UV 366 nm for the detection of ketone, aldehyde and alcohol functions corresponding mostly to carbohydrates.

2.5. Microfabrication

Microfluidic chips for fungal culture (Fig. 1) were fabricated by soft lithography as described by Baranger et al. (2020). The pattern was imprinted on a silicon wafer using two layers of SU8 photoresist (Microfactory, IPGG, Paris): a first layer comprised of the microchannel pattern with an average thickness of 5.8 ± 0.3 μm, and a second layer forming the culture chambers, with an average thickness of 124 ± 2 μm. Polydimethylsiloxane (PDMS, Sylgard 184, Dow Corning) mixed with 10% reticulating agent was cast against the wafer and allowed to cure for at least 2 h at 70 °C. Inlets were added by punching holes through the PDMS with a biopsy puncher (2 mm for the inoculation well, 1 mm for medium injection inlets). The negatively patterned PDMS slab was bound to a clean glass microscope slide or cover slip after surface oxidization in an oxygen plasma chamber (Harrick) for 60 s.

2.6. On-chip fungal culture

All chips were filled with sterile MMG prior to seeding with mycelium. A 2 mm diameter mycelium plug was collected from a solid-medium culture of *T. helicus* at the edge of the growing colony, and transferred to the inoculation inlet of the chip. The inlet was then closed with a PDMS plug to prevent drying. 1 μL of BaP stock solution (0.8 g/L in acetone) was pipetted into one of the injection inlets on the opposite side to the inoculation chamber right after inoculation. Upon contact with the aqueous culture medium, BaP immediately precipitated into crystals localized at the injection inlet. The microchips were then placed in a sealed Petri dish in a water-saturated atmosphere. The mycelium was allowed to grow at 22 °C with a 12 h - 12 h light-dark cycle in static conditions. Mycelial growth in the device and fluorescent staining of the cells due to BaP uptake were monitored in the chips for up to 8 days.

2.7. Microscopy imaging and image processing

Mycelia of *T. helicus* grown in liquid cultures with BaP and mounted between slide and coverslip were imaged in bright field and epifluorescence using an OLYMPUS BX60 microscope mounted with a color Infinity 3-6UR camera (Lumenera). Time-lapse epifluorescence

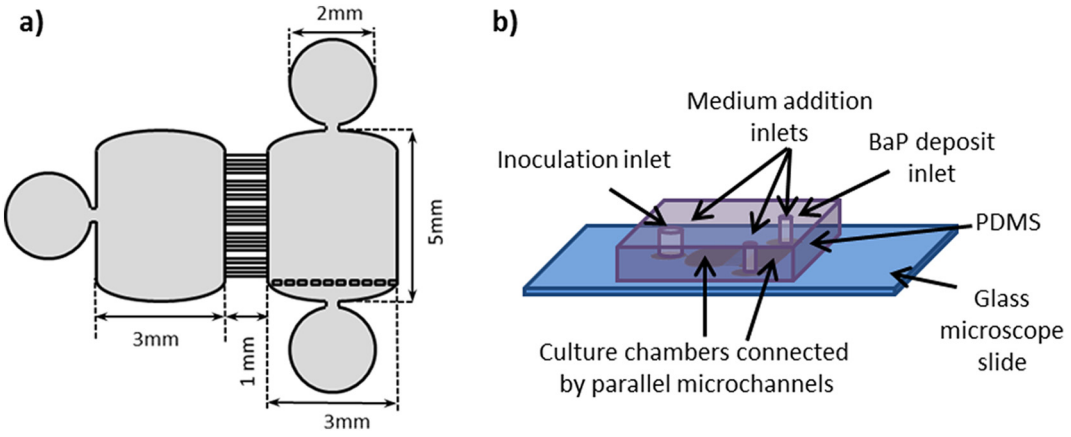

Fig. 1. Diagram representing the microfluidic device used for fungal cultivation in presence of BaP. a. Channel geometry. b. Experimental set-up.

microscopy observations were performed using a DMI-8 inverted microscope (Leica) equipped with a motorized stage and a DFC 3000G camera (Leica). The fluorescence of BaP was observed with a standard DAPI emission filter set.

Microchips inoculated with *T. helicus* and spiked with BaP were imaged using a confocal laser scanning microscope (LSM 710 Axio Observer, Carl Zeiss). The fluorescent signal of BaP was detected using the DAPI filter (excitation 405 nm, emission 453 nm) and that of BODIPY using the FITC filter (excitation 488 nm, emission 563 nm).

All image processing and measurements were carried out using ImageJ. For the BODIPY co-staining experiment, mycelium mounted on a glass slide was imaged in confocal microscopy at 40× magnification with z increments of 0.38 μm, and maximum intensity projections along z were made. For the on-chip fungal culture experiments, stacks of 11 images with a 1 μm increment were projected along z. Average grey intensity was measured over rectangular areas of 10 × 100 μm (12 × 121 pixels) in 3 separate microchannels on each image. Results are presented as mean and standard deviation of the 3 measurements for each time point.

2.8. In silico simulation

The penetration of BaP through a model lipid bilayer was simulated using the IMPALA method as first described by Ducarme et al. (1998). Briefly, this method is based on a Monte Carlo approach using an implicit description of membrane. The latter is described as a continuous medium whose properties vary along the axis perpendicular to the bilayer plane (z axis). The force field was parameterized to mimic a membrane in aqueous environment by considering (1) the hydrophobic effect between the membrane and a solute (Epho) and (2) the perturbation effect of the solute on the lipid acyl chain organization (Elip). The two restraints were calculated and summed at each position of BaP into the implicit membrane and the molecule was systematically moved along the z axis by 1 Å steps, from one side of the membrane to the other. The method yields a profile of the interaction energy for each position along the Z axis, the most stable positions being those with minimal energy.

3. Results

3.1. Benzo[a]pyrene diffusion in lipid phases

BaP is highly hydrophobic (log $K_{ow} = 6.35$) and has an extremely low solubility in water ($3.8 \cdot 10^{-3}$ mg/L at 25 °C) (IARC, 2012). This compound forms solid crystals when added to aqueous media such as those used for microbial cultures. In soil, it is associated to solid particles and organic matter, but can also be present in hydrocarbon mixtures as non-aqueous phase liquids (Ortega-Calvo et al., 2013).

The intracellular uptake of BaP in fungal cells implies that the molecule reaches cell surfaces and transport occurs through the plasma membrane. In order to predict the interaction of BaP with biological membranes, its penetration into an implicit symmetrical lipid bilayer was simulated by the IMPALA method (Fig. 2 a). As expected for a hydrophobic molecule, the profile displayed a sharp contrast between the positions corresponding to the water phase surrounding the membrane and those corresponding to the hydrocarbon core of the membrane. The most stable positions for BaP, displaying negative interaction energies, are located between −14 Å and 14 Å, and correspond to the alkyl core of the model lipid bilayer. In contrast, the interaction energy is maximal above −22 Å and 22 Å, and decreases sharply between (−)22 Å and (−)14 Å. This decrease coincides with positions where the BaP molecule is in contact with the membrane, and still partially surrounded by water. Indeed, for a 36 Å thick membrane, the hydrated phosphate heads of the amphiphilic lipids are located between 14 and 18 Å.

The energy profile obtained predicts that the BaP molecule is most stable at the core of lipid bilayers, This result is consistent with the low solubility in water of BaP, which tends to minimize its contact surface with aqueous phases.

3.2. Intracellular localization of benzo[a]pyrene in Talaromyces helicus

Since BaP emits a blue fluorescent signal when excited with UV light, its incorporation into the fungal biomass can be visualized directly through epifluorescence microscopy. Off-chip observations of *T. helicus* mycelium pellets incubated with BaP for 24 h were thus carried out. In control flasks without BaP, a slight fluorescence of the mycelium was visible under UV (Fig. 2 b). The fluorescent signal observed without addition of any fluorophore corresponds to the autofluorescence of parietal components. Indeed, fungal hyphae are known to emit blue autofluorescence when exposed to UV light (330–385 nm) due to the presence of chitin in the fungal wall (Jabaji-Hare et al., 1984; Dreyer et al., 2006).

After 24 h of incubation with BaP, the mycelium pellets appeared brightly fluorescent at their core, which could be due to the immediate contact with BaP crystals trapped in the hyphal network. Blue fluorescence was detected along hyphae, with cell walls and septa appearing more strongly stained than the cytoplasm. Many intracellular vesicles were visible in bright field, and appeared brightly fluorescent. In some hyphal tips, these vesicles were distributed in the cytoplasm. In mature hyphae, the vesicles were localized at the periphery of the cytoplasm, while vacuoles were not stained (Fig. 2 b). When mycelium previously incubated with BaP was stained with BODIPY and observed in confocal microscopy, blue and green fluorescent signals co-localized in lipid bodies indicating BaP intracellular storage in these organelles (Fig. 2 c).

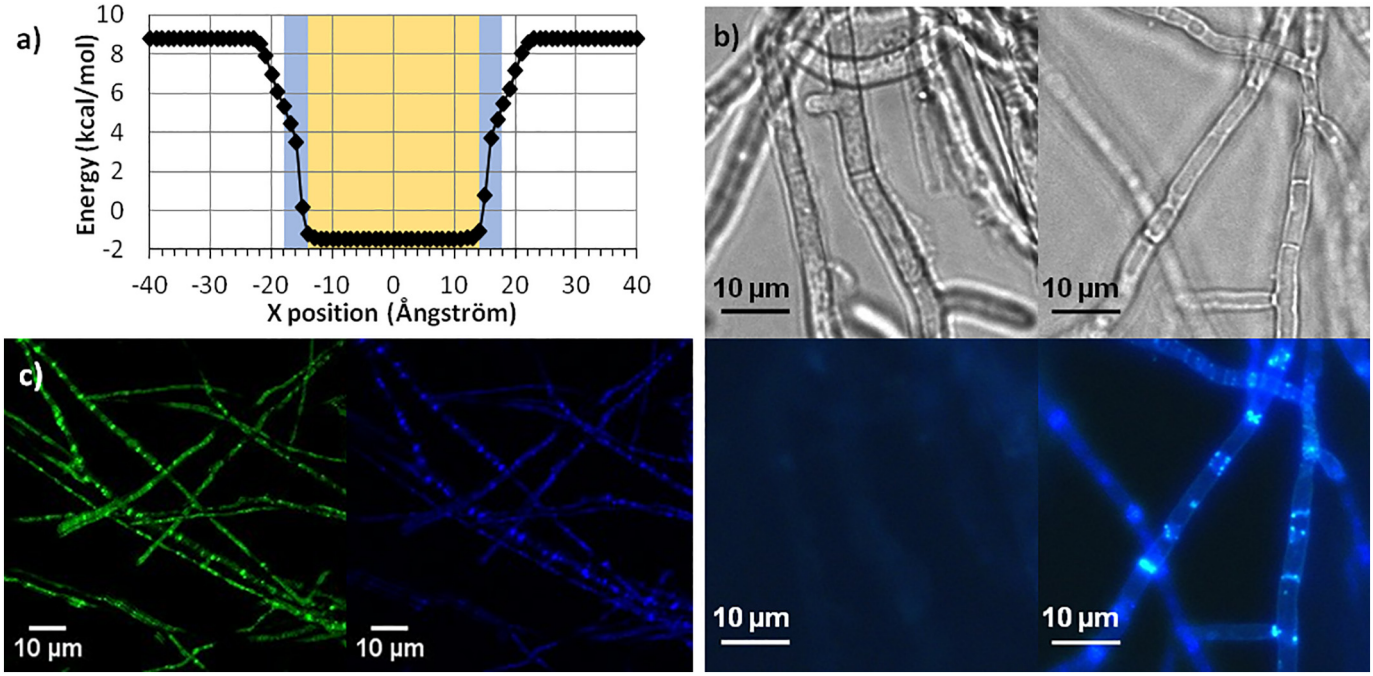

Fig. 2. a - Simulation of BaP penetration across a model lipid bilayer using the IMPALA method. X-axis: position of the mass center of BaP relatively to the center of the lipid bilayer; Y-axis: interaction energy calculated as described in Materials and methods. The different regions of the membrane are highlighted in yellow (core hydrocarbon chains) and blue (polar heads). b - Mycelium of *T. helicus* after 24 h of incubation with or without BaP, observed in bright field (top row) and epifluorescence using the DAPI excitation filter (bottom row). left: control mycelium without BaP, showing a faint cell wall autofluorescence; right: mycelium incubated with BaP, displaying small stained vesicles localized at the periphery of hyphal segments. c - Mycelium of *T. helicus* incubated with BaP and stained with BODIPY, observed in confocal microscopy at 40× magnification (maximum intensity projection of a 41 images stack with a 0.38 µm increment, false colors). Left: FITC filter (green); right: DAPI filter (blue). Both color channels show fluorescent staining colocalized in intracellular vesicles. (For interpretation of the references to color in this figure legend, the reader is referred to the web version of this article.)

3.3. Detection of fungal surface-active molecules

Culture filtrates of *T. helicus* were harvested and analyzed through surface tension measurements to detect potential fungal surfactants (Fig. 3 a). Surface tension in culture filtrates decreased over time and reached a minimum after 6 days, stabilizing until the end of the experiment (after 13 days). The surface tension was lowered to 49.4 ± 0 mN/m, compared to 69 ± 3.7 mN/m in fresh, sterile mineral medium. This result clearly demonstrates the presence of surface-active compounds in the extracellular medium. Extracellular proteins or biosurfactants secreted by the fungus may be responsible for this decrease.

In order to gather more information on the chemical nature of these surfactants, culture filtrates harvested after 13 days of incubation were analyzed in high performance thin-layer chromatography (Fig. 3 b). 13-day filtrates were chosen because they contain the lowest glucose contents, which can interfere with the results and make it difficult to concentrate the samples. After migration, six main spots were detected through 254 nm UV illumination, which reveals organic compounds in a

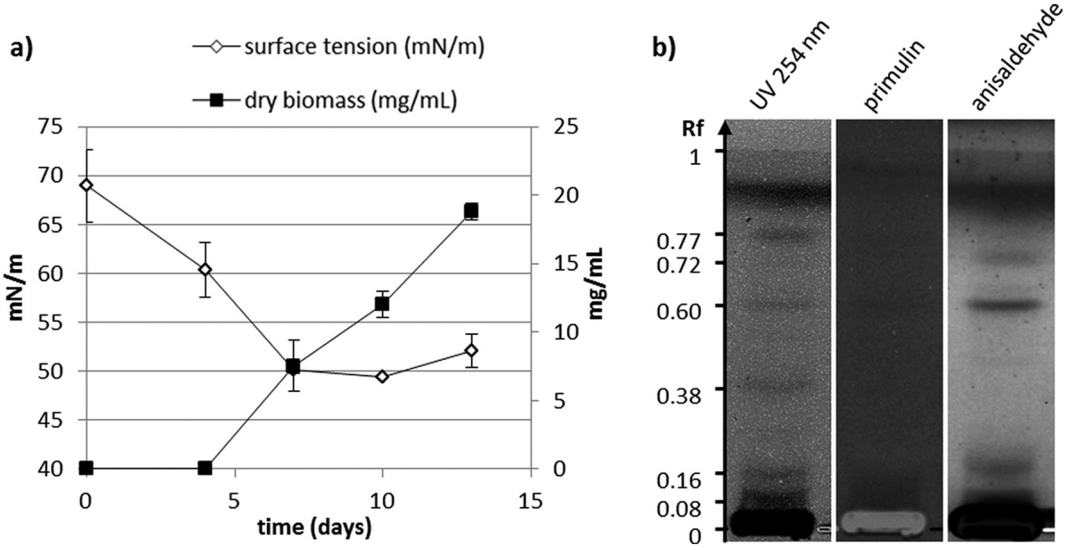

Fig. 3. Detection of surface-active compounds in culture supernatants of *T. helicus* grown in mineral medium. a - Surface tension of the cell-free supernatant and dry fungal biomass over time. b - HPTLC analysis of a 13-day supernatant sample. From left to right: observation under UV light at 254 nm to reveal organic compounds, after primulin staining to detect lipids at 366 nm, and after anisaldehyde staining to detect carbohydrates under white light.

non-specific way. The most intense spot was detected at 0.05 Rf and corresponds to residual glucose in the sample. Five fainter spots were detected at 0.08, 0.16, 0.38, 0.60 and 0.77 Rf. After spraying with a primulin solution to detect lipids and imaging at 266 nm, the only visible spot corresponded to the migration coefficient of glucose. Finally, anisaldehyde revelation was used to reveal carbohydrates. Spots at 0.08, 0.16, 0.60 Rf and the glucose spot reacted with anisaldehyde, but not the spots appearing at 0.60 and 0.77 Rf. In addition, a new spot at 0.72 Rf was visible in white light with anisaldehyde revelation. This compound may be present in concentrations too low for the spot to be visible without prior staining.

The filtrate is a mixture of several compounds with various affinities with the organic phase, which appears to be predominantly made of carbohydrates, and not lipids. Peptides were not investigated in HPTLC, however protein quantification in the filtrates through the Bradford method show the presence of extracellular protein in low amounts with the highest concentration at 3 mg/L after 10 days of incubation.

3.4. Benzo[a]pyrene mobilization in a compartmentalized device

T. helicus was grown in microfluidic chips spiked with BaP, and the mycelium was observed at different growth stages. The mycelium was imaged in bright field to monitor growth and locate the edge of the colony. Chips were then observed in laser scanning confocal microscopy to detect the fluorescent staining of hyphae due to BaP incorporation.

Fig. 4 a shows the evolution of the fluorescent staining over time at two observations points in the same chip: in chamber A close to the inoculum (left column) and in chamber B right at the opening of microchannels (right column). Fig. 4 b represents the position of the different elements within the chip geometry. The intensity of the fluorescent staining increased over time. After 4 days of incubation, the mycelium had grown into the inoculation chamber A but did not yet reach chamber B. Faint and diffuse staining of the hyphae was observed, but not more intense than the natural autofluorescence of the mycelium observed in control chips without BaP. After 5 days, hyphae reached the channels but not BaP crystals yet and the mycelium fluorescence appears still low. After 6 days and even more after 7 days, staining intensity clearly increased and was not uniform across the mycelium, i.e. single stained hyphae were distinguishable and appeared more brightly fluorescent than others in contrast to the control (Fig. 4 a). No distinct stained vesicles were visible at 20× magnification. Microchannels enabled the quantification of grey intensity over time in the same area (Fig. 4 c). The average fluorescence intensity appears to increase between 3 and 5 days, whereas it remains stable in the control over the whole experiment, which evokes a BaP uptake before direct contact between hyphae and BaP crystals occurred. However the difference of grey intensities between test with BaP and control starts to be statistically significant after 7 days when direct contact between the mycelium and the BaP deposit occurs.

In order to better locate the fluorescence within hyphae, several chips were observed at greater magnification (40×) after 6 and 7 days. Growth velocity was greatly variable from one chip to the other, as previously assessed in the same device with this fungal strain (Baranger et al., 2020). As a result, after 7 days of incubation the mycelium had not reached the BaP deposit in all of the chips (Fig. 5 a and b). In some of the chips where direct contact happened, staining of the mycelium was detected in chamber B. Stained apices were observed at the growth front, in close vicinity to the deposit (Fig. 5 c). In these apices, no lipid bodies were distinguishable and the whole cytoplasm appeared fluorescent. This could be due to the presence of numerous, closely packed lipid droplets that could not be resolved with the camera used. Indeed, the resolution of the images was 0.21 μm/pixel at 40× magnification, while some of the lipid droplets detected in stained apices with the Lumenera camera (used for epifluorescence images) could be as small as 0.2 μm. In mature, ramified hyphae located in the chamber, and directly in contact with the crystals, stained vesicles were clearly visible (Fig. 5 d). Some hyphae in the microchannels were stained as well (not shown). The stained structures were similar to those observed in mycelium grown in liquid medium supplemented with BaP, as described in Section 3.2.

Interestingly, in chips imaged before the mycelium had reached the deposit, fluorescent staining different from mycelia grown without BaP was observed as well. Indeed, faintly stained apices were visible at the growth front of the mycelium growing through the microchannels (Fig. 5 a). Some hyphae localized in chamber B, closer to the BaP deposit, displayed a stronger staining and visible intracellular lipid bodies (Fig. 5 b). The cell wall and some septa appeared to be stained as well. The stained lipid bodies were smaller and less numerous than they were in hyphae in contact with BaP crystals (Fig. 5 d).

4. Discussion

4.1. Benzo[a]pyrene storage in lipid bodies

Epifluorescence observations with a co-staining with BODIPY confirm that BaP is absorbed into the cells of *T. helicus* and stored in lipid bodies. Similar observations were made in the saprotrophic fungus *Fusarium solani* (Verdin et al., 2005; Fayeulle et al., 2014) as well as other fungal strains including the yeast *Saccharomyces cerevisiae*, the white rot *Phanerochaete chrysosporium* (Verdin et al., 2005), and the oomycete *Pythium ultimum* (Furuno et al., 2012). Intracellular PAH uptake thus appears to occur in several fungal species regardless of PAH degradation efficiency.

Accumulation of lipophilic toxins in lipid bodies may be a defense mechanism against oxidative stress in fungi. Indeed, Chang et al. (2015) found that the formation of large lipid bodies in *Candida albicans* was associated with mycotoxin resistance, and that toxins were stored in lipid bodies. The authors propose a protection mechanism against oxidative stress caused by the oxidation of aromatic rings, involving quenching of reactive oxygen species by the triacyglycerols making up the bulk of storage lipids. A similar strategy in *Talaromyces helicus* may serve as a protection against the adverse effects of BaP and other lipophilic organic compounds.

Additionally, lipid bodies may be a site of intracellular degradation. Delsarte et al. (2018) proposed a connection between BaP degradation and neutral lipid cycling in fungal cells, hypothesizing that BaP stored in lipid bodies could be oxidized simultaneously as lipid beta-oxidation occurs in neighboring peroxisomes.

4.2. Preferential uptake at a close range

Previous hypotheses on the uptake mechanisms of hydrophobic compounds suggest that growing hyphal tips, which are metabolically active and host intense exchanges with the extracellular environment, are preferential sites of uptake (Fayeulle et al., 2014). In accordance with this hypothesis, mycelium incubated with BaP frequently displays stained hyphal tips. Transport and storage in older parts of the mycelium is suspected but not established. Indeed, stained lipid bodies are visible in all parts of the mycelium, indicating that BaP is either incorporated in already formed segments, or brought there from the tips through intrahyphal transport. Intrahyphal translocation of PAH through vesicle streaming was observed in *P. ultimum* (Furuno et al., 2012). However, although cytoplasmic streaming was observed during our time-lapse experiments in bright field microscopy, no evidence of lipid body movement was found in *T. helicus* with specific staining. Previous studies suggest that lipid bodies in filamentous fungi originate from the endoplasmic reticulum, forming small lipid bodies that later fuse into larger ones (Kamisaka et al., 1999). Such early precursors of the mature lipid bodies may be more mobile, but smaller than the camera resolution used for the present experiments. Alternatively, BaP could be solubilized in membranes and be transported along with vesicles to various organelles, in a similar way to neutral lipids and other

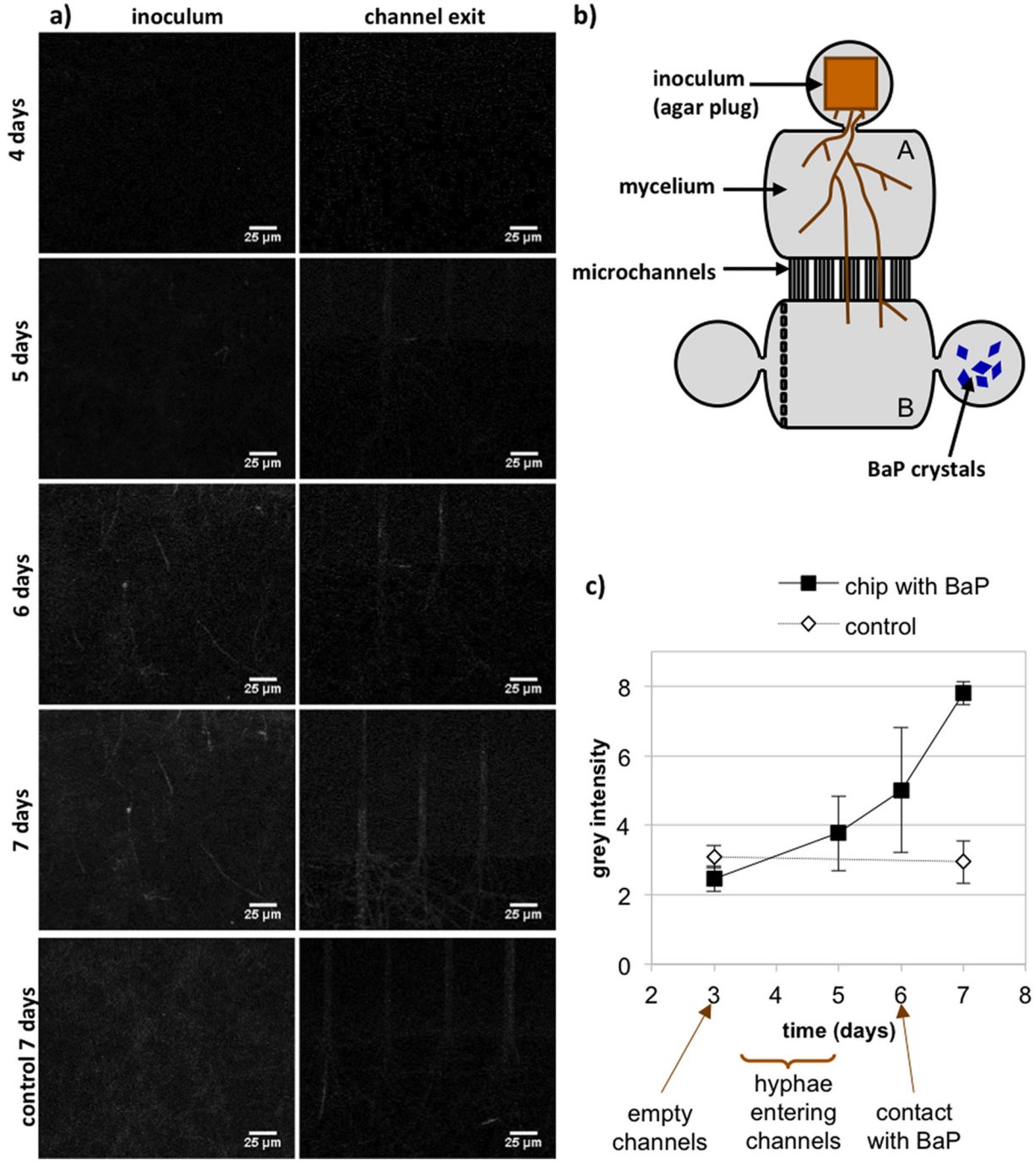

Fig. 4. a. Mycelium of *T. helicus* growing in a microfluidic chip spiked with BaP, observed in LSCM at 20× magnification (maximal intensity projection of image stacks with a 1 µm increment). Left column: Images taken in chamber A (inoculum). Right column: Images taking at the opening of microchannels on the side of chamber B (BaP deposit). b. Diagram representing the microfluidic device used for fungal cultivation in presence of BaP. c. Variation of fluorescence intensity over time, as represented by the average grey intensity measured in three microchannels in the same microchip over a 10 × 100 µm area (error bars represent the standard deviation of each triplicate; arrows indicate the grey intensity of empty channels, the hyphae entrance in channels and the time after which the direct contact between mycelium and BaP occurred in the considered chip).

lipophilic compounds (Murphy et al., 2009). Indeed, the IMPALA simulation results predict that the most stable position for BaP in a lipid bilayer is within the hydrophobic core, which indicate a possible penetration into cell membranes and subsequent lateral diffusion. The insertion of PAH into model lipid membranes was also demonstrated experimentally (Castelli et al., 2002). However it is very unlikely for BaP in the molecular form to be present in water surrounding cells and to diffuse freely through the extracellular aqueous medium at concentrations high enough to explain its effective biodegradation. Thus for BaP to be absorbed into membranes, it would need to be already in close vicinity to the cell surface, either as crystals, or solubilized by surface-active molecules. Transport phenomena, other than passive diffusion, must therefore occur earlier than the cell membrane crossing in the incorporation process to bring the pollutant in contact with the cell surface.

Microscopic observations of *T. helicus* in spiked microfluidic chips indicate a preferential uptake of BaP at a close range and through contact with the cell wall. Indeed, when BaP is supplied as a fixed solid deposit

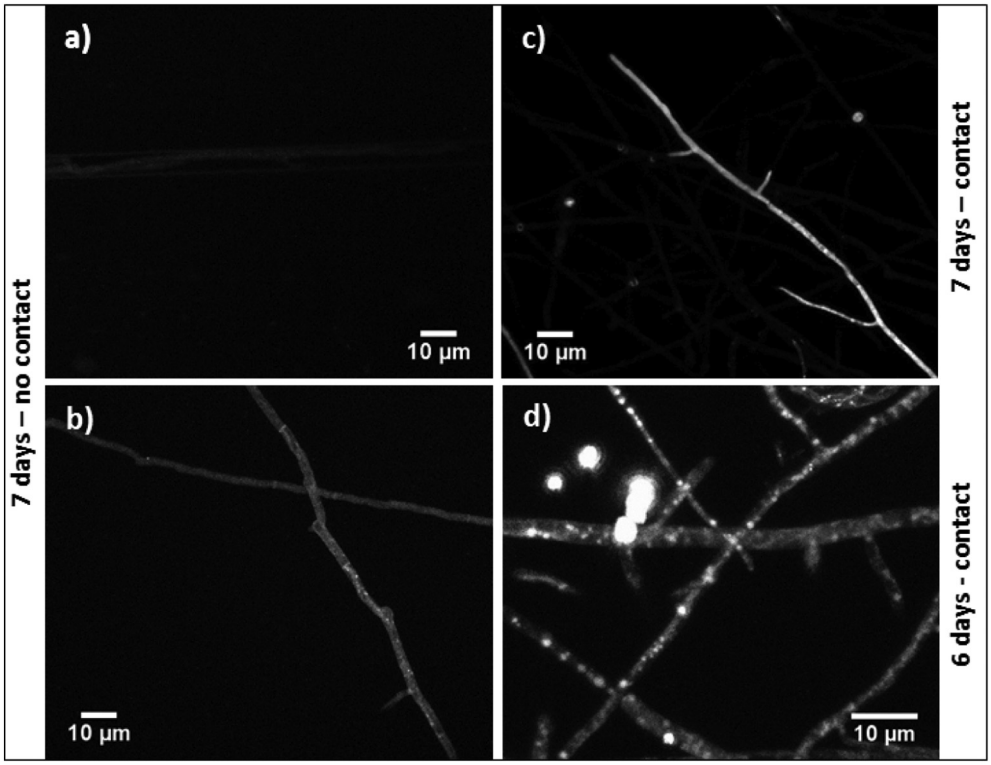

Fig. 5. Mycelium of *T. helicus* growing in microfluidic chips spiked with BaP, observed in LSCM at 40× magnification after 6 to 7 days of incubation. (maximum intensity projection of image stacks with a 1 µm increment). a. Detail of hyphae growing in a microchannel before the mycelium reached the BaP deposit – b. Detail of hyphae growing in chamber B. after the mycelium grew through the channels but not yet reached the BaP deposit. c. Stained hyphal tips in chamber B, close to the BaP deposit. d. Hyphae displaying stained intracellular lipid bodies in chamber B, in direct contact with BaP crystals.

in microfluidic chambers, fluorescent staining of the mycelium is the most intense after the deposit has been reached. This is consistent with observations in mycelium suspensions as well, since, when BaP crystals are dispersed in the liquid medium through continuous agitation, they can come into direct contact with hyphae and get trapped into the tightly knit mycelial network. As a result, the core of mycelial pellets frequently appears brightly stained as opposed to growing hyphae at the periphery. Moreover, early staining of some hyphae was observed before contact with BaP crystals in microfluidic chips. The staining was most often localized in some hyphal apices, sometimes highlighting the cell wall of older hyphae and lipid bodies in the cytoplasm. These results indicate that a long-range mobilization mechanism is at play, bringing BaP molecules to the fungal cells before hyphae could reach the solid crystals. The staining of cell walls observed on some occasions suggests that BaP adsorption to cell walls is a preliminary step to further internalization. Accumulation of BaP at the cell wall was previously shown in *F. solani* (Fayeulle et al., 2014) when the formation of actin filaments is inhibited, preventing endocytosis and vesicle trafficking. In a context of non-inhibited metabolic activity, little to no staining of the cell wall is observed, indicating an equilibrium between cell wall adsorption rates and uptake rates.

4.3. Extracellular mobilization and transport

The access to the BaP deposits in crystal form relies either on hyphal growth up to the source, or on transport in water. Surface-active compounds may increase BaP partitioning into the water phase by accumulating at the surface of solid BaP particles and promote their fragmentation and dispersion in the medium. This hypothesis seems in accordance with the observation that surfactants enable transfers of hydrophobic molecules between hydrophobic phases of an emulsion stabilized by solid particles (Drelich et al., 2012). However, the possible role of fungal surfactants in BaP mobilization has not been elucidated so far.

The mechanisms involved in hydrophobic pollutant mobilization could be closely linked to the nutrition behaviour of filamentous fungi. Indeed, hydrophobic compounds in contaminated soils such as BaP are frequently associated with non-aqueous phase liquids and organic matter, which can readily be used by fungi as carbon sources. Some microbial surfactants are able to partially solubilize hydrophobic organic compounds (Ron and Rosenberg, 2002; Van Hamme et al., 2006), including PAH (Garcia-Junco et al., 2003; Sánchez-Vázquez et al., 2018), thus enhancing their bioavailability. Sophorolipid biosurfactants excretion has also been linked to the degradation of anthracene sorbed to a solid matrix in several yeast species (Romero et al., 2016). However in our study with *Talaromyces helicus*, no extracellular lipids were detected, excluding sophorolipids or other similar glycolipids from biosurfactants candidates. Interestingly, non-lipidic surface-active molecules have been described to play major roles in fungal interactions with hydrophobic substrates such as hydrophobins (Berger and Sallada, 2019) or exopolysaccharides (Mahapatra and Banerjee, 2013). This kind of molecules could be related to the surface tension decrease of culture filtrates observed in our study. Dissolved organic matter itself can serve as a mobilizing agent promoting hydrophobic organic compounds (HOC) dispersion in the water phase (Smith et al., 2009, 2011). Biosurfactants could also promote the dispersal and transport of small solid particles or droplets of organic phases containing BaP. Additionally, fungal hyphae whose growth was oriented towards the source of nutrients following a gradient, may thus come into contact with associated pollutants. Facilitated transport of HOC in small amounts in the aqueous phase would thus be a preliminary step to direct contact and incorporation in greater amounts.

Although the main PAH biodegradation pathway in non-ligninolytic fungi is thought to be intracellular, fungi release a variety of

extracellular enzymes involved in nutrition, including oxidoreductases such as laccases, lignin peroxidases, manganese peroxidases, and tyrosinases which catalyze the production of oxidizing agents and free radicals leading to the non-specific oxidation of substrates (Tuomela and Hatakka, 2011). The fungal metabolism of aromatic compounds produces substituted derivatives that are more reactive and more soluble than the original pollutants like phenol, phthalate, hydroxyl-, carboxy- and dihydrodiol derivates that may in a second step be conjugated with sugar moieties (Boll et al., 2015; Marco-Urrea et al., 2015). Such metabolites display radically different behaviors compared to the parent PAHs, and tend to partition into the water phase at much higher rates, which could promote their absorption by micro-organisms and facilitate their transport through the cell membrane.

4.4. Fungal access to benzo[a]pyrene in compartmentalized environments

Taken together our results enable to propose a two-steps mechanism for the access to BaP by a non-ligninolytic fungus before its uptake and intracellular biodegradation in a compartmentalized microenvironment like soil. Firstly, a distant uptake was shown, which highlights an extracellular mobilization step possibly related to the surface-active agents detected in filtrates or to extracellular enzyme activities. This first step may increase the presence of BaP or associated hydrophobic compounds in the water phase and create gradients susceptible to drive growth to the pollutant source. Secondly uptake appears to be more efficient after the mycelium touches a BaP deposit, which could be explained by a better access to the pollutant through a direct chemical partitioning between BaP crystals and hydrophobic portions of the hyphae surfaces as suggested by the simulation. These mechanisms of mobilization and uptake could vary according to the physicochemical properties of the considered PAH and in particular its water solubility. Indeed the phenanthrene and BaP uptakes by *F. solani* showed different kinetics and were suggested to occur through different mechanisms (Fayeulle et al., 2014). The better understanding of these active phenomena to reach hydrophobic pollutants is of relevance to enhance mycoremediation efficiency though biostimulation approaches, since low PAH bioavailability remains one of the major limitations for the development of these techniques (Akhtar and Mannan, 2020). The elucidation of the mechanisms by which filamentous fungi influence PAH bioavailability in soils (Posada-Baquero et al., 2019) and transport these molecules through the hyphal network (Harms et al., 2011) are also important to understand how they can positively interact with other types of organisms within combined bioremediation strategies (Baranger et al., 2021). Notably positive results in bioremediation of PAH impacted soils have been obtained through combination of mycoremediation and phytoremediation (Ma et al., 2021).

5. Conclusion

A compartmentalized microchip was designed to observe the incorporation of benzo[*a*]pyrene by the fungus *Talaromyces helicus* in a controlled geometry. This is the first time to our knowledge that BaP fungal uptake is directly observed in a compartmentalized system and that a combination of extracellular surfactants and direct contact uptake is proposed to explain this phenomenon. Indeed the fungus is able to develop a mycelium in the confined chambers, and hyphae can grow in direct contact with BaP crystals. Observations through epifluorescence and confocal microscopy confirmed that the pollutant is incorporated into the cells of *T. helicus*, and co-staining experiments with BODIPY lipid dye show that lipid bodies are a preferential storage site in the cell. BaP uptake in *T. helicus* occurred even when hyphae were not directly touching the crystals, but to a lower extent than when hyphae were in direct contact with the crystals. Additionally, *T. helicus* produces extracellular surface-active compounds that were detected in culture filtrates. Thus, the use of a microfluidic device in our study brings first pieces of evidence for a two-steps mechanism involved in the access to BaP by a non-ligninolytic soil fungus before its uptake and intracellular biodegradation.

Fundings

C.B. benefited from a doctoral grant from the French Ministry of Research. The MycoFlu project has been supported by grants from the CNRS (EC2CO programme MICROBIEN) and Sorbonne Universités (programme Emergence, SU-16-R-EMR-28).

CRediT authorship contribution statement

Claire Baranger: Conceptualization, Data curation, Formal analysis, Investigation, Methodology, Visualization, Writing – original draft. **Isabelle Pezron:** Investigation, Methodology, Resources, Supervision, Writing – review & editing. **Laurence Lins:** Data curation, Investigation, Methodology, Resources, Software, Writing – review & editing. **Magali Deleu:** Data curation, Investigation, Methodology, Resources, Software, Writing – review & editing. **Anne Le Goff:** Conceptualization, Formal analysis, Funding acquisition, Investigation, Methodology, Project administration, Resources, Supervision, Validation, Writing – review & editing. **Antoine Fayeulle:** Conceptualization, Formal analysis, Funding acquisition, Investigation, Methodology, Project administration, Resources, Supervision, Validation, Writing – original draft, Writing – review & editing.

Declaration of competing interest

The authors declare that they have no known competing financial interests or personal relationships that could have appeared to influence the work reported in this paper.

Acknowledgements

The authors would like to thank Sandrine Lelong-Caristan and the society Chromacim for their support in HPTLC analyses. The authors are also grateful to Xue Sun, Alicia Alejandra Mier Gonzalez, Marie Valmori, Roxane Valentin and Théo Guillerm for their help with the preliminary experiments.

References

Akhtar, N., Mannan, M.A., 2020. Mycoremediation: expunging environmental pollutants. Biotechnol. Rep. 26, e00452. https://doi.org/10.1016/j.btre.2020.e00452.

Aleklett, K., Kiers, E.T., Ohlsson, P., Shimizu, T.S., Caldas, V.E., Hammer, E.C., 2018. Build your own soil: exploring microfluidics to create microbial habitat structures. ISME J. 12, 312–319. https://doi.org/10.1038/ismej.2017.184.

Al-Hawash, A.B., Zhang, X., Ma, F., 2019. Removal and biodegradation of different petroleum hydrocarbons using the filamentous fungus *Aspergillus* sp. RFC-1. Microbiol. Open 8, e00619. https://doi.org/10.1002/mbo3.619.

Alnahhas, R.N., Winkle, J.J., Hirning, A.J., Karamched, B., Ott, W., Josić, K., Bennett, M.R., 2019. Spatiotemporal dynamics of synthetic microbial consortia in microfluidic devices. ACS Synth. Biol. 8, 2051–2058. https://doi.org/10.1021/acssynbio.9b00146.

Arutchelvi, J.I., Bhaduri, S., Uppara, P.V., Doble, M., 2008. Mannosylerythritol lipids: a review. J. Ind. Microbiol. Biotechnol. 35, 1559–1570. https://doi.org/10.1007/s10295-008-0460-4.

Baranger, C., Fayeulle, A., Le Goff, A., 2020. Microfluidic monitoring of the growth of individual hyphae in confined environments. R. Soc. Open Sci. 7, 191535. https://doi.org/10.1098/rsos.191535.

Baranger, C., Pezron, I., Le Goff, A., Fayeulle, A., 2021. Fungal influence on hydrophobic organic pollutants dynamics within the soil matrices. In: Kumar, V. (Ed.), Rhizomicrobe Dynamics in Bioremediation. CRC Press, pp. 1–27 https://doi.org/10.1201/9780367821593-1 ISBN 9780367419660, 2021, Chapter 1.

Berger, B.W., Sallada, N.D., 2019. Hydrophobins: multifunctional biosurfactants for interface engineering. J. Biol. Eng. 13, 10. https://doi.org/10.1186/s13036-018-0136-1.

Boll, E.S., Johnsen, A.R., Christensen, J.H., 2015. Polar metabolites of polycyclic aromatic compounds from fungi are potential soil and groundwater contaminants. Chemosphere 119, 250–257. https://doi.org/10.1016/j.chemosphere.2014.06.033.

Castelli, F., Librando, V., Sarpietro, M.G., 2002. Calorimetric approach of the interaction and absorption of polycyclic aromatic hydrocarbons with model membranes. Environ. Sci. Technol. 36, 2717–2723. https://doi.org/10.1021/es010260w.

Cerniglia, C.E., Sutherland, J.B., 2010. Degradation of polycyclic aromatic hydrocarbons by fungi. In: Timmis, K.N. (Ed.), Handbook of Hydrocarbon and Lipid Microbiology. Springer Berlin Heidelberg, Berlin, Heidelberg, pp. 2079–2110.
Chang, W., Zhang, M., Zheng, S., Li, Y., Li, X., Li, W., Li, G., Lin, Z., Xie, Z., Zhao, Z., Lou, H., 2015. Trapping toxins within lipid droplets is a resistance mechanism in fungi. Sci. Rep. 5, 1–11. https://doi.org/10.1038/srep15133.
Črešnar, B., Petrič, Š., 2011. Cytochrome P450 enzymes in the fungal kingdom. BBA Proteins Proteom. 1814, 29–35. https://doi.org/10.1016/j.bbapap.2010.06.020.
Delsarte, I., Rafin, C., Mrad, F., Veignie, E., 2018. Lipid metabolism and benzo[a]pyrene degradation by *Fusarium solani*: an unexplored potential. Environ. Sci. Pollut. Res. 25, 12177–12182. https://doi.org/10.1007/s11356-017-1164-y.
Drelich, A., Grossiord, J.-L., Gomez, F., Clausse, D., Pezron, I., 2012. Mixed O/W emulsions stabilized by solid particles: a model system for controlled mass transfer triggered by surfactant addition. J. Colloid Interface Sci. 386, 218–227. https://doi.org/10.1016/j.jcis.2012.07.072.
Dreyer, B., Morte, A., Pérez-Gilabert, M., Honrubia, M., 2006. Autofluorescence detection of arbuscular mycorrhizal fungal structures in palm roots: an underestimated experimental method. Mycol. Res. 110, 887–897. https://doi.org/10.1016/j.mycres.2006.05.011.
Ducarme, Ph., Rahman, M., Brasseur, R., 1998. IMPALA: a simple restraint field to simulate the biological membrane in molecular structure studies. Proteins 30, 357–371.
Fayeulle, A., 2013. Etude des mécanismes intervenant dans la biodégradation des Hydrocarbures Aromatiques Polycycliques par les champignons saprotrophes telluriques en vue d'applications en bioremédiation fongique de sols pollués. Université du Littoral Côte d'Opale, Dunkerque.
Fayeulle, A., Veignie, E., Slomianny, C., Dewailly, E., Munch, J.-C., Rafin, C., 2014. Energy-dependent uptake of benzo[a]pyrene and its cytoskeleton-dependent intracellular transport by the telluric fungus *Fusarium solani*. Environ. Sci. Pollut. Res. 21, 3515–3523. https://doi.org/10.1007/s11356-013-2324-3.
Fayeulle, A., Veignie, E., Schroll, R., Munch, J.C., Rafin, C., 2019. PAH biodegradation by telluric saprotrophic fungi isolated from aged PAH-contaminated soils in mineral medium and historically contaminated soil microcosms. J. Soils Sediments 19, 3056–3067. https://doi.org/10.1007/s11368-019-02312-8.
Furuno, S., Foss, S., Wild, E., Jones, K.C., Semple, K.T., Harms, H., Wick, L.Y., 2012. Mycelia promote active transport and spatial dispersion of polycyclic aromatic hydrocarbons. Environ. Sci. Technol. 46, 5463–5470. https://doi.org/10.1021/es300810b.
Garay, L.A., Sitepu, I.R., Cajka, T., Xu, J., Teh, H.E., German, J.B., Pan, Z., Dungan, S.R., Block, D.E., Boundy-Mills, K.L., 2018. Extracellular fungal polyol lipids: a new class of potential high value lipids. Biotechnol. Adv. 36, 397–414.
Garcia-Junco, M., Gomez-Lahoz, C., Niqui-Arroyo, J.-L., Ortega-Calvo, J.-J., 2003. Biosurfactant- and biodegradation-enhanced partitioning of polycyclic aromatic hydrocarbons from nonaqueous-phase liquids. Environ. Sci. Technol. 37, 2988–2996. https://doi.org/10.1021/es020197q.
Grossmann, G., Guo, W.-J., Ehrhardt, D.W., Frommer, W.B., Sit, R.V., Quake, S.R., Meier, M., 2011. The RootChip: an integrated microfluidic chip for plant science. Plant Cell 23, 4234–4240. https://doi.org/10.1105/tpc.111.092577.
Harms, H., Schlosser, D., Wick, L.Y., 2011. Untapped potential: exploiting fungi in bioremediation of hazardous chemicals. Nat. Rev. Microbiol. 9, 177–192. https://doi.org/10.1038/nrmicro2519.
Held, M., Lee, A.P., Edwards, C., Nicolau, D.V., 2010. Microfluidics structures for probing the dynamic behaviour of filamentous fungi. Microelectron. Eng. 87, 786–789. https://doi.org/10.1016/j.mee.2009.11.096.
Huang, L.H., Schmitt, J.A., 1975. Ohio ascomycete notes II. *Talaromyces* from soils of southern Ohio. Ohio J. Sci. 75, 75–81.
IARC - International Agency for Research on Cancer - Working Group on the Evaluation of Carcinogenic Risks to Humans, 2012. Benzo[a]pyrene. In : Chemical Agents and Related Occupations. IARC Monographs on the Evaluation of Carcinogenic Risks to Humans, Lyon, France, pp. 111–144.
Jabaji-Hare, S.H., Perumalla, C.J., Kendrick, W.B., 1984. Autofluorescence of vesicles, arbuscules, and intercellular hyphae of a vesicular–arbuscular fungus in leek (*Allium porrum*) roots. Can. J. Bot. 62, 2665–2669.
Jennings, A.A., 2012. Worldwide regulatory guidance values for surface soil exposure to carcinogenic or mutagenic polycyclic aromatic hydrocarbons. J. Environ. Manag. 110, 82–102. https://doi.org/10.1016/j.jenvman.2012.05.015.
Kamisaka, Y., Noda, N., Sakai, T., Kawasaki, K., 1999. Lipid bodies and lipid body formation in an oleaginous fungus, *Mortierella ramanniana* var. *angulispora*. BBA Mol. Cell Biol. L. 1438, 185–198. https://doi.org/10.1016/S1388-1981(99)00050-5.
Käppeli, O., Walther, P., Mueller, M., Fiechter, A., 1984. Structure of the cell surface of the yeast *Candida tropicalis* and its relation to hydrocarbon transport. Arch. Microbiol. 138, 279–282. https://doi.org/10.1007/BF00410890.
Kuppusamy, S., Thavamani, P., Venkateswarlu, K., Lee, Y.B., Naidu, R., Megharaj, M., 2017. Remediation approaches for polycyclic aromatic hydrocarbons (PAHs) contaminated soils: technological constraints, emerging trends and future directions. Chemosphere 168, 944–968. https://doi.org/10.1016/j.chemosphere.2016.10.115.
Leriche-Grandchamp, M., Flourat, A., Shen, H., Picard, F., Giordana, H., Allais, F., Fayeulle, A., 2020. Inhibition of phenolics uptake by ligninolytic fungal cells and its potential as a tool for the production of lignin-derived aromatic building blocks. J. Fungi 6, 362. https://doi.org/10.3390/jof6040362.
Lindley, N.D., Heydeman, M.T., 1986. Mechanism of dodecane uptake by whole cells of *Cladosporium resinae*. Microbiology 132, 751–756. https://doi.org/10.1099/00221287-132-3-751.
Ma, X., Li, X., Liu, J., Cheng, Y., Zou, J., Zhai, F., Sun, Z., Han, L., 2021. Soil microbial community succession and interactions during combined plant/white-rot fungus remediation of polycyclic aromatic hydrocarbons. Sci. Total Environ. 752, 142224. https://doi.org/10.1016/j.scitotenv.2020.142224.
Mahapatra, S., Banerjee, D., 2013. Fungal exopolysaccharide: production, composition and applications. Microbiol. Insights 6, 1–16. https://doi.org/10.4137/MBI.S10957.
Marco-Urrea, E., García-Romera, I., Aranda, E., 2015. Potential of non-ligninolytic fungi in bioremediation of chlorinated and polycyclic aromatic hydrocarbons. New Biotechnol. Eur. Congr. Biotechnol. ECB 16 32, 620–628. https://doi.org/10.1016/j.nbt.2015.01.005.
Moore, D., Robson, G.D., Trinci, A.P.J., 2015. 21st Century Guide to Fungi. Cambridge University Press.
Murphy, S., Martin, S., Parton, R.G., 2009. Lipid droplet-organelle interactions; sharing the fats. BBA Mol. Cell Biol. L. 1791, 441–447. https://doi.org/10.1016/j.bbalip.2008.07.004.
Olagoke, O.A., 2014. Amylase activities of some thermophilic fungi isolated from municipal solid wastes and palm-kernel stack. Am. J. Microbiol. Biotechnol. 1, 64–70.
Ortega-Calvo, J.J., Tejeda-Agredano, M.C., Jimenez-Sanchez, C., Congiu, E., Sungthong, R., Niqui-Arroyo, J.L., Cantos, M., 2013. Is it possible to increase bioavailability but not environmental risk of PAHs in bioremediation? J. Hazard. Mater. 261, 733–745. https://doi.org/10.1016/j.jhazmat.2013.03.042.
Panagos, P., Van Liedekerke, M., Yigini, Y., Montanarella, L., 2013. Contaminated sites in Europe: review of the current situation based on data collected through a european network. J. Environ. Pub. Health 2013, 1–11. https://doi.org/10.1155/2013/158764.
Posada-Baquero, R., Martín, M.L., Ortega-Calvo, J.-J., 2019. Implementing standardized desorption extraction into bioavailability-oriented bioremediation of PAH-polluted soils. Sci. Total Environ. 696, 134011. https://doi.org/10.1016/j.scitotenv.2019.134011.
Puchkov, E.O., Zähringer, U., Lindner, B., Kulakovskaya, T.V., Seydel, U., Wiese, A., 2002. The mycocidal, membrane-active complex of *Cryptococcus humicola* is a new type of cellobiose lipid with detergent features. BBA Biomembranes 1558, 161–170. https://doi.org/10.1016/S0005-2736(01)00428-X.
Rayu, S., Karpouzas, D.G., Singh, B.K., 2012. Emerging technologies in bioremediation: constraints and opportunities. Biodegradation 23, 917–926. https://doi.org/10.1007/s10532-012-9576-3.
Romero, M.C., Hammer, E., Hanschke, R., Arambarri, A.M., Schauer, F., 2005. Biotransformation of biphenyl by the filamentous fungus *Talaromyces helicus*. World J. Microb. Biot. 21, 101–106. https://doi.org/10.1007/s11274-004-2779-y.
Romero, M.C., Urrutia, M.I., Reinoso, E.H., Moreno Kiernan, A., 2009. Wild soil fungi able to degrade the herbicide isoproturon. Rev. Mex. Micol. 29, 1–7.
Romero, M.C., Urrutia, M.I., Reinoso, H.E., Kiernan, M.M., 2010. Benzo[a]pyrene degradation by soil filamentous fungi. J. Yeast Fungal Res. 1, 025–029.
Romero, M.C., Chiaravalli, J.C., Reinoso, E.H., 2016. Sorbed anthracene degradation by sophorolipid producing yeasts. Int. J. Biotech Well. Indus. 5 (25-31–31).
Ron, E.Z., Rosenberg, E., 2002. Biosurfactants and oil bioremediation. Curr. Opin. Biotechnol. 13, 249–252. https://doi.org/10.1016/S0958-1669(02)00316-6.
Sánchez-Vázquez, V., Shirai, K., González, I., Gutiérrez-Rojas, M., 2018. Polycyclic aromatic hydrocarbon-emulsifier protein produced by *Aspergillus brasiliensis* (*niger*) in an airlift bioreactor following an electrochemical pretreatment. Bioresour. Technol. 256, 408–413. https://doi.org/10.1016/j.biortech.2018.02.043.
Scervino, J.M., Mesa, M.P., Della Mónica, I., Recchi, M., Sarmiento Moreno, N., Godeas, A., 2010. Soil fungal isolates produce different organic acid patterns involved in phosphate salts solubilization. Biol. Fertil. Soil 46, 755–763. https://doi.org/10.1007/s00374-010-0482-8.
Smith, K.E.C., Thullner, M., Wick, L.Y., Harms, H., 2009. Sorption to humic acids enhances polycyclic aromatic hydrocarbon biodegradation. Environ. Sci. Technol. 43, 7205–7211. https://doi.org/10.1021/es803661s.
Smith, K.E.C., Thullner, M., Wick, L.Y., Harms, H., 2011. Dissolved organic carbon enhances the mass transfer of hydrophobic organic compounds from nonaqueous phase liquids (NAPLs) into the aqueous phase. Environ. Sci. Technol. 45, 8741–8747. https://doi.org/10.1021/es202983k.
Squires, T.M., Quake, S.R., 2005. Microfluidics: fluid physics at the nanoliter scale. Rev. Mod. Phys. 77, 977–1026. https://doi.org/10.1103/RevModPhys.77.977.
Tuomela, M., Hatakka, A., 2011. Oxidative fungal enzymes for bioremediation. Industrial and Toxic Wastes. Elsevier, pp. 183–196.
Van Hamme, J.D., Singh, A., Ward, O.P., 2006. Physiological aspects: part 1 in a series of papers devoted to surfactants in microbiology and biotechnology. Biotechnol. Adv. 24, 604–620. https://doi.org/10.1016/j.biotechadv.2006.08.001.
Verdin, A., Lounès-Hadj Sahraoui, A., Newsam, R., Robinson, G., Durand, R., 2005. Polycyclic aromatic hydrocarbons storage by *Fusarium solani* in intracellular lipid vesicles. Environ. Pollut. 133, 283–291. https://doi.org/10.1016/j.envpol.2004.05.040.
Vidali, M., 2001. Bioremediation. An overview. Pure Appl. Chem. 73, 1163–1172. https://doi.org/10.1351/pac200173071163.
Wilpiszeski, R.L., Aufrecht, J.A., Retterer, S.T., Sullivan, M.B., Graham, D.E., Pierce, E.M., Zablocki, O.D., Palumbo, A.V., Elias, D.A., 2019. Soil aggregate microbial communities: towards understanding microbiome interactions at biologically relevant scales. Appl. Environ. Microbiol. 85, e00324-19. https://doi.org/10.1128/AEM.00324-19.
Wu, H., Wu, L., Wang, J., Zhu, Q., Lin, S., Xu, J., Zheng, C., Chen, J., Qin, X., Fang, C., Zhang, Z., Azeem, S., Lin, W., 2016. Mixed phenolic acids mediated proliferation of pathogens *Talaromyces helicus* and *Kosakonia sacchari* in continuously monocultured *Radix pseudostellariae* rhizosphere soil. Front. Microbiol. 7, 335. https://doi.org/10.3389/fmicb.2016.00335.